

Full Research Paper

Evaluation of Grassland Dynamics in the Northern-Tibet Plateau of China Using Remote Sensing and Climate Data

Jiahua Zhang ^{*1}, Fengmei Yao ², Lingyun Zheng ¹ and Limin Yang ³

1 Laboratory for Remote Sensing and Climate Information Sciences (LRSCIS), Chinese Academy of Meteorological Sciences, Beijing, 100081, China; E-mail: zhangjh@cma.cma.gov.cn.

2 College of Earth Sciences, The Graduate University of the Chinese Academy of Sciences, Beijing, 100049, China; E-mail: yaofm@gucas.ac.cn

3 Visiting Scientist, U.S. Geological Survey, Center for Earth Resources Observation and Science, Sioux Falls, South Dakota, 57198, USA

* Author to whom correspondence should be addressed.

Received: 13 October 2007 / Accepted: 14 December 2007 / Published: 17 December 2007

Abstract: The grassland ecosystem in the Northern-Tibet Plateau (NTP) of China is very sensitive to weather and climate conditions of the region. In this study, we investigate the spatial and temporal variations of the grassland ecosystem in the NTP using the NOAA/AVHRR ten-day maximum NDVI composite data of 1981-2001. The relationships among Vegetation Peak-Normalized Difference Vegetation Index (VP-NDVI) and climate variables were quantified for six counties within the NTP. The notable and uneven alterations of the grassland in response to variation of climate and human impact in the NTP were revealed. Over the last two decades of the 20th century, the maximum greenness of the grassland has exhibited high increase, slight increase, no-change, slight decrease and high decrease, each occupies 0.27%, 8.71%, 77.27%, 13.06% and 0.69% of the total area of the NTP, respectively. A remarkable increase (decrease) in VP-NDVI occurred in the central-eastern (eastern) NTP whereas little change was observed in the western and northwestern NTP. A strong negative relationship between VP-NDVI and ET_0 was found in sub-frigid, semi-arid and frigid-arid regions of the NTP (i.e., Nakchu, Shantsa, Palgon and Amdo counties), suggesting that the ET_0 is one limiting factor affecting grassland degradation. In the temperate-humid, sub-frigid and sub-humid regions of the NTP (Chali and Sokshan counties), a significant inverse correlation between VP-NDVI and population indicates that human activities have adversely affected the grassland condition as was previously reported in the literature. Results from this research suggest that the alteration

and degradation of the grassland in the lower altitude of the NTP over the last two decades of the 20th century are likely caused by variations of climate and anthropogenic activities.

Keywords: Grassland dynamic, NOAA/AVHRR, Northern-Tibet Plateau, Climate change, Human activities.

1. Introduction

The Northern-Tibet Plateau (NTP) covers a vast territory of the western China with an average altitude of 4,500 m. Also known as the roof of the world and the third pole of the earth, it is the source of the ancient and modern glaciers as well as the source of many large rivers in China such as the Yangtze, the Yellow, the Nujiang and the Lancang Rivers [1-3]. The NTP plays an important role as the thermal forcing to the atmospheric circulation in Asia. The thermal state of the NTP links closely to the regional weather and climate condition, such as temperature, precipitation regime, and the status of the monsoon [1, 4].

Grassland of the NTP is the third largest grassland ecosystem in China, covering 90% of the total land surface of NTP [2, 5]. The NTP is ecologically fragile and is more sensitive to the global climate change as compared to the other part of the world [1, 6]. For instance, the annual mean temperature of the NTP has risen at a rate of 0.4°C/decade over the most recent 40 years, which is much higher than that of other parts of China and the rest of the world [7]. In addition, the surface area of many lakes in the NTP has decreased over time. For example, the area of surface water of the Namu Lake (the biggest lake of the NTP) has decreased by 38.58 km² from year 1970 to 1988, with a decreasing rate of 2.14 km²/year [8].

Land use activity represents the most substantial human alteration of the earth for a long period [9]. The pace, magnitude and spatial extent of the human alterations over the last 300 years are unprecedented. In recent years, with the development of economy and increasing population, the grassland ecosystem has rapidly degraded and grassland area has decreased [2, 10]. It is generally believed that the occurrence and expansion of grassland degradation due to acidification and desertification over the NTP are closely related to changes in climate, ecological condition and human activity, such as overgrazing, excessively timber cutting and digging [2,3,11]. In addition, the NTP has been one of the major sources of the sand storms that have occurred in China [12].

Since 1970s, earth observing satellites have become a unique tool with which one can objectively monitor status and changes of the terrestrial ecosystems at the regional and global scales, and for ecological, geographical, meteorological and environmental studies [13-18]. One important sensor on-board the National Oceanic and Atmospheric Administration (NOAA)'s series of satellites is the Advanced Very High Resolution Radiometer (AVHRR), which records spectral data that are useful for monitoring the terrestrial environment [19-24], land use and land cover changes [25-33], and the interaction between the terrestrial ecosystem and climate [34-40].

Pervious studies reported that climate change has affected the inter-annual variations of vegetation conditions and grassland dynamics [41-44]. In recent years, under the dual influences of natural and human factors, a large expanse of grassland in the NTP region has seriously degraded [2, 10]. The

drier and warmer climate in the NTP and its surrounding areas has also aggravated desertification and soil erosion. The grassland productivity has also declined greatly and become a huge obstacle to the sustainable social, economic and ecological development. Despite the ecological significance of the region, until now, little research has been carried out to study the long-term grassland dynamics and the driving forces. In this study, we investigate the spatial and temporal variations and possible causes of the grassland ecosystem in the NTP using a 19-year time series of the Normalized Difference Vegetation Index (NDVI) data and corresponding climate and demographic data.

2. The study area

The NTP region lies within 29°55' -36°30' N, and 83°55' -95°05' E (see Fig. 1). It covers approximately 395,400 km² and is composed of eleven counties. The total area of the NTP accounts for 32.82% of the total land area, and 41.65% of the total grassland of the Tibetan Autonomous Region of China.

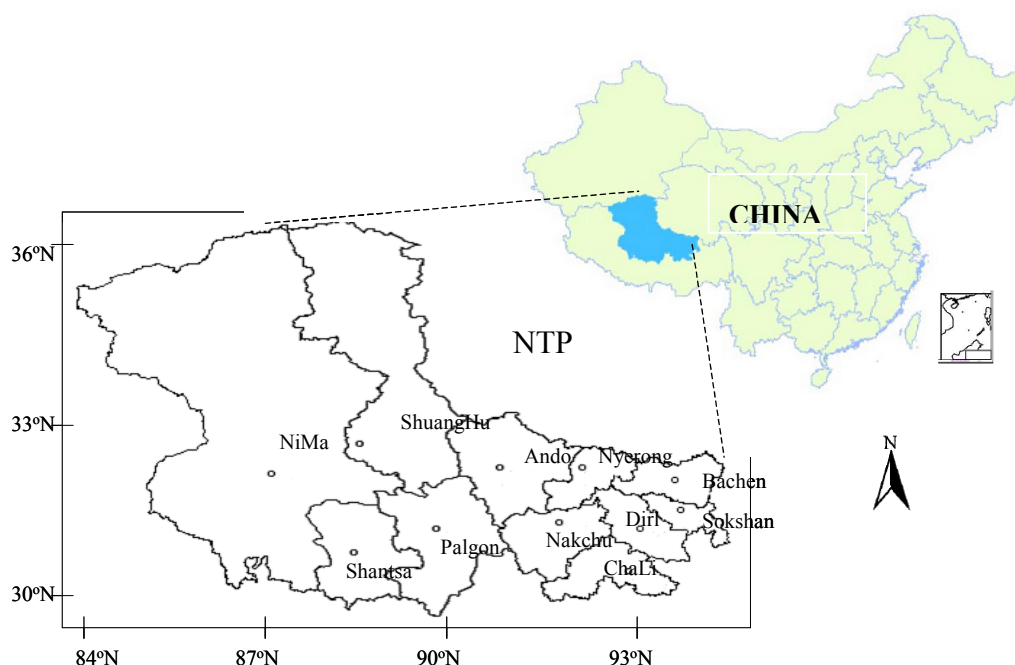


Figure 1 Study area. The NTP is located in the South-western of China with elevation above 4,500 m.

In the NTP region, the annual mean temperature ranges between -2.9° and 3.4°C, and the annual precipitation between 298.6 and 708.4 mm. Affected by the atmospheric circulation and local terrain, about 80% of the total precipitation occurs in between June and September, and the amount of precipitation declines from the east to west and from the south to north. Snow usually occurs from the October to April. The annual evaporation ranges from 1,500 -2,300 mm, increasing from the southeast to northwest [2, 10, 44]. The duration of sunshine in a typical year averages more than 2,852 hours [8].

Geographically, four climatic zones can be delineated in the NTP region: temperate-humid, sub-frigid sub-humid, sub-frigid semi-arid, and frigid arid zones [45]. Corresponding to these climatic zones, four major native pasturelands are identified from the southeast to northwest: bush-meadow,

alpine meadow, alpine grassland, and desert grassland. The dominant forage plants of the usable pastures belong to Cyperaceae and Gramineae, with Compositae, Leguminosae, and Rosaceae occurring as the subdominants. The composition of pastures in the east and central part of the region is complex due to variations in climate and local terrain; the grassland becomes less complex botanically towards the northwest where the altitude is higher and the climate is harsher. The growing season typically extends from May through September, with a growing period of less than 150 days. The population in the NTP region is approximately 376,800 (2003 census). Farmers in this region are primarily engaged in animal husbandry except for a few who produce grain crops in the eastern counties. Tibetan sheep, goats, and yak are the dominant livestock for many enterprises with some horses and cattle.

3. Data and methodology

3.1 Satellite data processing and statistical analysis

The NOAA-AVHRR Pathfinder data set is a ten-day maximum NDVI composite derived from the NOAA-7, -9, -11 and -14 satellite images with radiometrically and geometrically correction and a spatial resolution of 8 km × 8 km [46-47]. The NDVI composite of 1981 -2001(except for 1994) is used in this study. The maximum NDVI compositing reduces the effects of atmospheric aerosols, water vapor, high scan angles, higher solar zenith angles and residual cloud contamination [48].

The NDVI is an indicator related to absorbed photosynthetic active radiation by vegetation and it has been widely used to estimate green biomass, leaf area index (LAI) and productivity of vegetation. The formula used to compute NDVI is:

$$NDVI = \frac{NIR - Red}{NIR + Red} \quad (1)$$

where *NIR* (AVHRR Channel 2: 0.725 ~1.1 μm) and *Red* (AVHRR Channel 1: 0.58 ~0.68 μm) are spectral reflectance of the near infrared and red portion of the electromagnetic spectrum, respectively. The construction of the NDVI is based on the fact that the internal mesophyll structure of the healthy green leaves strongly reflects near infrared radiation whereas the leaf chlorophyll and other pigments absorb a large proportion of the radiation in visible (red) spectrum [14-15].

The NDVI ranges from -1.0 to 1.0, where negative values correspond to an absence of vegetation [49]. In this study, the third generation product (AVHRR PAL) of NDVI is used, which has been rescaled to a range of 0 to 254. Figure 2 displays the average annual maximum NDVI of the NTP.

For the study site, an average of maximum NDVI for July, August and September over each 3 × 3 64-km² (9 pixel block) was calculated. In addition, an average annual NDVI of the peak growing season (VP-NDVI) was computed for each of every 19-year and study site by taking the average of the maximum NDVI of July, August and September.

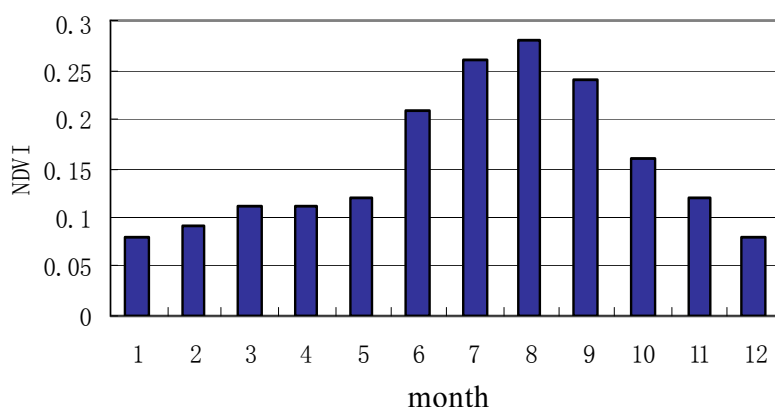


Figure 2. Monthly average NDVI in the NTP from 1981 to 2001

A linear trend and slope of the VP-NDVI time series was then calculated using the least-square method as follows [50]:

$$b = \frac{n \sum_{i=1}^n x_i y_i - \sum_{i=1}^n x_i \sum_{i=1}^n y_i}{n \sum_{i=1}^n x_i^2 - (\sum_{i=1}^n x_i)^2} \quad (2)$$

where, b is the slope of the trend, x_i is the year and y_i is the NDVI in the i^{th} year. A negative regression coefficient indicates a decline of VP-NDVI and a positive regression coefficient indicates an increase of VP-NDVI. Figure 3 depicts the regression coefficients pixel-by-pixel for the entire NTP.

The pattern of VP-NDVI trend from 1981 to 2001 as shown in Figure 3 resembles a normal distribution, ranging from -0.15 to 0.15.

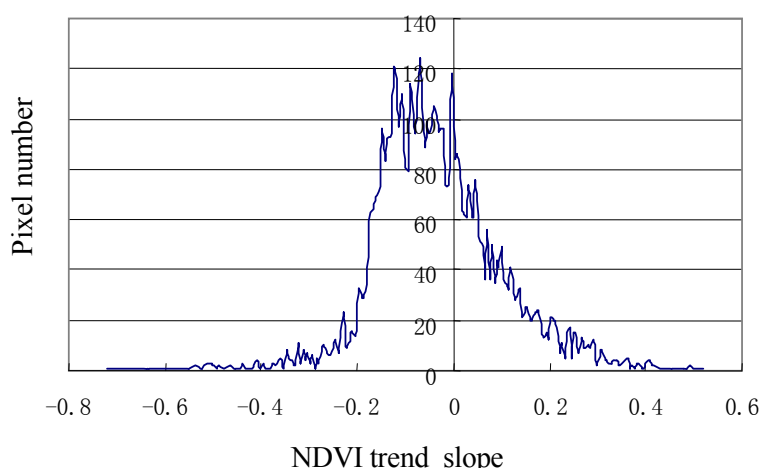


Figure 3. Trends in VP-NDVI change in the NTP region from 1981 to 2001.

This VP-NDVI trend is hypothesized as the natural fluctuation of land surface in the NTP. The gain coefficient values of all pixels in the NTP were classified into five-levels that describe changes of VP-NDVI over the 19-year period. The five levels are: high increase (> 0.41 VP-NDVI unites over the 20 years); slight increase (between 0.15 and 0.41 VP-NDVI unites); no change (within ± 0.15 VP-NDVI

unites); slight decrease (between -0.15 and -0.41 VP-NDVI unites); and high decrease (< - 0.41 VP-NDVI unites).

3.2 Climate data processing

Climate data of 1981-2001 were collected for six weather stations in the NTP (see Table1). For each station, the data set includes surface air temperature, maximum temperature (T_{\max}), minimum temperature (T_{\min}), precipitation, wind speed and direction, atmospheric humidity, sunshine duration, and evaporation. The potential evapotranspiration (ET_0) is calculated by using Penman-Monteith equation [51] expressed as:

$$ET_0 = \frac{0.408\Delta(Rn - G) + \gamma \frac{900}{T + 272} u_2 (e_s - e_a)}{\Delta + \gamma(1 + 0.34u_2)} \quad (3)$$

where R_n is the net radiation, G is the soil heat flux, T is mean daily air temperature at 2 m height, u_2 is wind speed at 2 m height, e_s and e_a are the saturation vapor pressure and actual vapor pressure respectively, $e_s - e_a$ represents the saturation vapor pressure deficit, Δ is slope vapor pressure curve, γ is the psychrometric constant.

The correlation coefficient (R) was calculated between the VP-NDVI and each climate variables (i.e., T_{\max} , T_{\min} , precipitation, evaporation, wind speed, sunshine duration, and ET_0) using linear regression.

Table 1. General Information of six weather stations in the NTP.

Station names	Longitude (°E)	Latitude (°N)	Altitud e (m)	Annual mean precipitation (mm)	Annual mean temperature(°C)
Nakchu	92.1	31.5	4,508	428.9	-1.30
Shantsa	88.6	31.0	4,674	298.6	-2.90
Palgon	90.0	31.4	4,701	320.6	-0.05
Amdo	91.1	32.4	4,801	435.3	-2.80
Sokshan	93.8	31.9	4,024	572.3	1.60
Chali	93.3	30.7	4,489	708.4	-0.90

4. Result and discussion

4.1. Spatial and temporal patterns of VP-NDVI of the grassland in the NTP

The average VP-NDVI varies spatially and is primarily associated with different vegetation cover in the NTP (see Figure 4).

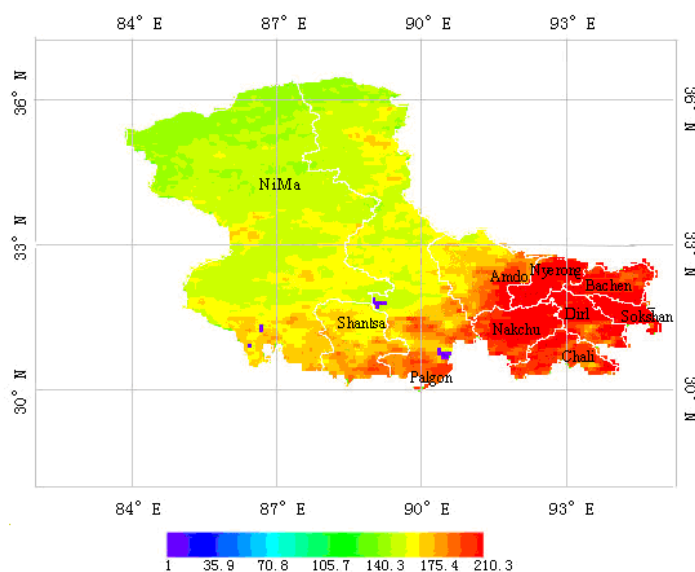


Figure 4. Spatial distribution of average VP-NDVI of grassland in NTP region from 1981 to 2001.

The largest VP-NDVI (>180) appears in area of relatively low elevation at the eastern NTP, with the major land use and cover being farmland, forest, bush- and alpine-meadow. In the central part of the NTP, the maximum VP-NDVI ranged from 160 to 180; In contrast, the maximum VP-NDVI falls in between 140 and 160 in the western part of the area, with sparsely-covered alpine steppe and desert steppe.

Analyses of the linear trend of VP-NDVI show that area with no or little change in PV-NDVI accounts for 77.27% of the total area of the NTP, whereas area with a high increase and slight increase accounts for 0.27% and 8.71%, respectively. Area with high decrease and slight decrease accounts for 0.69% and 13.06%, respectively (see Table 2).

Table 2. Statistic of VP-NDVI long-term trend (1981 – 2000) in the NTP. Five levels of change based on the linear trend coefficients of the VP-NDVI time series. Pixel number is the total number of pixels with VP-NDVI change (or no-change) that fall within each level of changes. Proportion is the number of changed (or no-change) pixels divided by the total number of pixels that fall within each level of change.

Trend in VP-NDVI	Trend line coefficients value	Pixel number	Proportion
High increase	>0.41	16	0.27%
Slight increase	0.15~0.41	516	8.71%
No change	-0.15~0.15	4,578	77.27%
Slight decrease	-0.41~-0.15	774	13.06%
High decrease	<-0.41	41	0.69%

Figure 5 illustrated the linear trends of VP-NDVI for each 64-km² pixel in the NTP, 1981 - 2001. Geographically, the increase and decrease in VP-NDVI occurred mainly in the eastern NTP at low altitude, whereas such trend was rather weak in the western NTP at the high altitude.

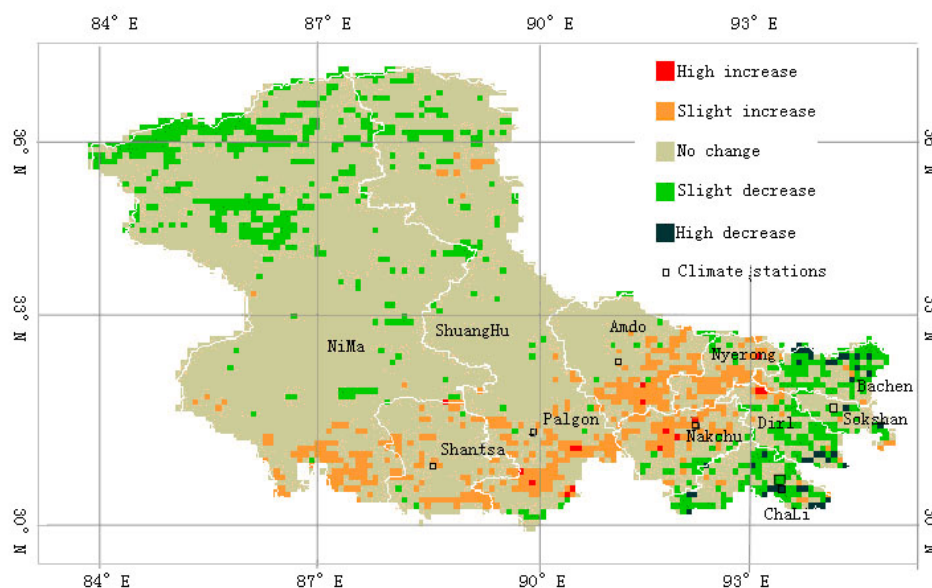


Figure 5. The linear trends of VP-NDVI of the NTP between 1981 and 2001.

4.2 NDVI and Climate driving force

4.2.1 NDVI-climate (temperature, precipitation, evaporation, wind, sunshine duration)

Figure 6 showed that mean annual temperature increased as recorded by all six weather stations which located in the NTP between 1981 and 2001. Liu and Chen also found that annual mean temperature increased in the Tibetan Plateau during 1955–1996 periods at a rate of 0.16 °C/decade, and the winter mean temperature also increased by 0.32 °C/decade [52]. These changes exceed those observed at the same latitudinal zone over the same time period.

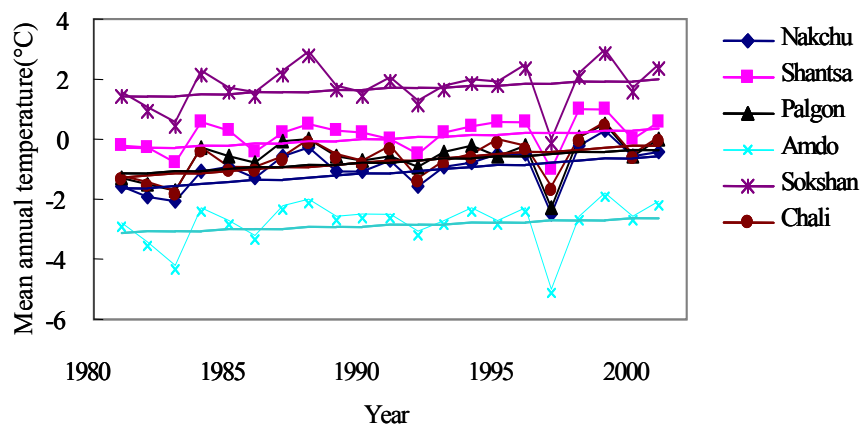


Figure 6. Mean annual temperature of six weather stations of NTP between 1981 and 2001.

As was shown in Figure 5, the linear trend of VP-NDVI varied spatially from the southern to central, and to the western NTP between 1981 and 2001. Table 3 listed several statistics, including the slope of the VP-NDVI trend, the annual precipitation trend, and the annual evaporation trend from 1981 to 2001 for each of the six weather stations. The results showed that annual precipitation increased at all six stations of NTP whereas the annual evaporation declined.

Table 3. VP-NDVI trend slope and annual precipitation trend slope in six stations between 1981 and 2001. b_v is VP-NDVI trend slope, b_p and b_E are the annual precipitation and evaporation trend slopes calculated based on equation 2.

Stations	Nakchu	Shantsa	Palgon	Amdo	Sokshan	Chali
b_v	0.409	0.238	0.058	-0.018	-0.069	-0.161
b_p	4.354	5.881	0.067	1.678	0.427	4.799
b_E	-10.390	-4.380	-9.340	-15.640	-0.360	-8.370

Generally, the grassland type in six stations of the NTP can be classified into bush meadow, alpine meadow, alpine grassland and desert grassland. A positive correlation between monthly VP-NDVI and monthly precipitation was observed for all six stations (see Table 4), which indicated that the precipitation is one of the dominant factor controlling seasonal variation of the grassland in the NTP.

Table 4. The correlation coefficient (R) between monthly VP-NDVI and monthly precipitation.

Station	Nakchu	Shantsa	Palgon	Amdo	Sokshan	Chali
Vegetation	alpine	alpine	alpine	alpine	bush	bush
type	meadow	grassland	grassland	meadow	meadow	meadow
Altitude	4,508	4,674	4,701	4,801	4,024	4,489
(m)	0.81*	0.67*	0.86*	0.74*	0.77*	0.71*
R						

* Correlation is significant at 0.01 level

Figure 7 illustrated a linear relationship between annual mean precipitation and average VP-NDVI for the six stations from 1981 to 2001. A higher annual mean precipitation correlates to higher VP-NDVI. The increase in VP-NDVI (y) can be related to the increase in precipitation (x):

$$y = 8.7338x - 1037.7 \quad (R^2=0.4196) \quad (3)$$

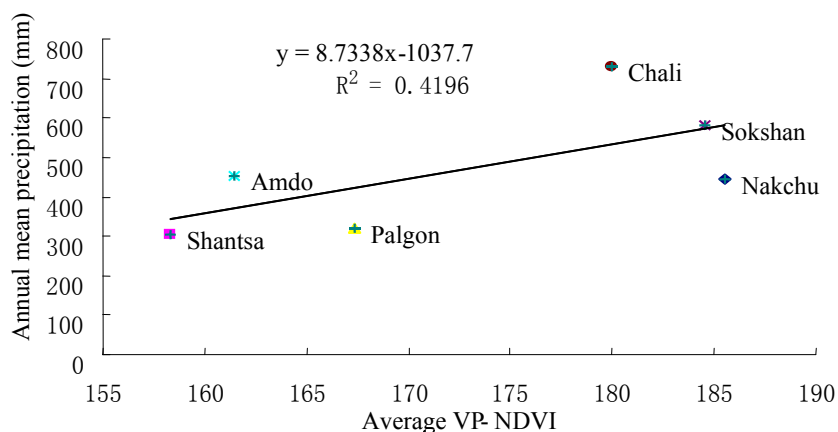


Figure 7. Annual mean precipitation and average VP-NDVI for the six weather stations of the NTP, 1981-2001.

Figure 8 showed that the annual mean wind speed decreased in six stations of the NTP from 1981 to 2001. In NTP region, the wind is important effecting factor for the grass growth, with declining of wind in this area, the grassland degradation trend was decreased. Furthermore, changes in wind speed, and to a lesser degree, relative humidity were among the most important factors affecting evaporation on the NTP. Therefore, the evaporation showed decline in six stations of NTP from 1981 to 2001 (see Table 3).

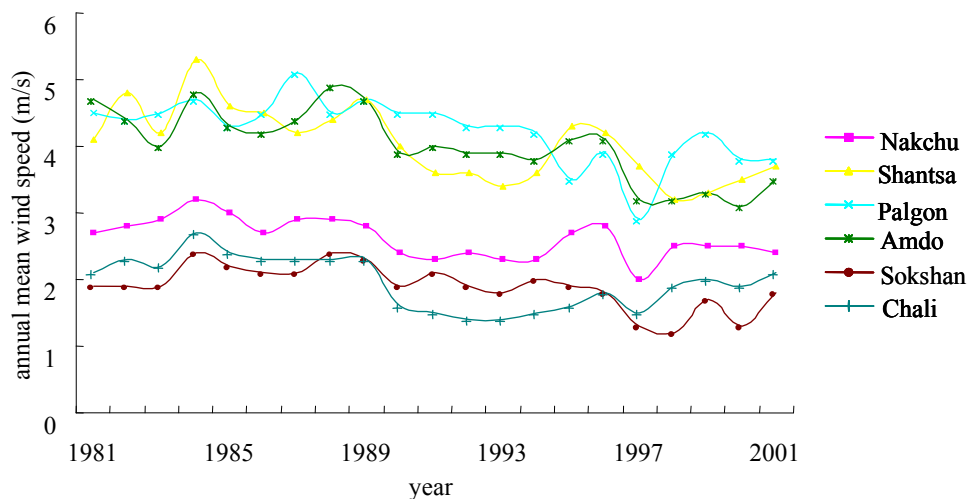


Figure 8. The annual mean wind speed in six counties of the NTP between 1981 and 2001.

The correlation coefficients (R) among the VP-NDVI and climate variables (i.e., T_{max} , T_{min} , precipitation during July to September, wind speed, sunshine duration during July to September, and ET_0) for six weather stations in the NTP were shown in Table 5.

Table 5. The correlation coefficient (R) between VP-NDVI and climate variables in six weather stations of the NTP.

R		Nakchu	Shantsa	Palgon	Amdo	Sokshan	Chali
T_{\min}		0.51*	-0.26	0.08	0.47*	0.27	-0.06
T_{\max}		0.21	-0.04	-0.19	-0.12	0.28	0.40
Precipitation	from July to September	0.33	0.39	0.17	0.10	0.53*	-0.15
ET_0		-0.63**	-0.51*	-0.63**	-0.54*	-0.07	0.29
Sunshine duration	from July to September	-0.71**	-0.44*	-0.47*	-0.60**	-0.24	0.17
Annual mean wind speed		-0.28	-0.40	-0.25	-0.19	0.21	0.03

* Correlation is significant at 0.05 level

** Correlation is significant at 0.01 level

The negative correlations between VP-NDVI and sunshine duration (from July to September) were also found in Nakchu station ($R = -0.71$, $p < 0.01$), Shantsa ($R = -0.44$, $p < 0.05$), Palgon ($R = -0.47$, $p < 0.05$), Amdo ($R = -0.60$, $p < 0.01$) and Sokshan ($R = -0.24$) (see Table 5).

4.2.2 VP-NDVI-climate relationship by counties

Nakchu County

In Nakchu County, the slope of VP-NDVI trend ($b_v = 0.409$), and the annual precipitation trend ($b_p = 4.354$) are positive (see Table 3), indicating that both NDVI and annual precipitation have increased over the twenty year time period. Besides, the correlation coefficient between T_{\min} and VP-NDVI in Nakchu county is 0.51 ($p < 0.05$), suggesting that minimum temperature is one of the limiting factors on the growth of over-wintered perennial grass [2, 7]. The negative correlation between VP-NDVI and ET_0 in Nakchu County ($R = -0.63$, $p < 0.01$) indicated the benefits of decreasing potential ET to the vegetation growth.

Chali County

Chali County is located in the sub-frigid sub-humid zone. The positive correlation between VP-NDVI and T_{\max} ($R = 0.40$) suggested that higher temperature is advantageous for grass growth in this sub-frigid sub-humid area. The weak negative correlation between VP-NDVI and precipitation during grass growth period (from July to September) ($R = -0.15$) indicated that precipitation is seem not a limited factor effecting grass growth in this sub-humid zone (the annual mean precipitation is 708.4 mm, which is the highest in six weather station in the NTP, also see from Table 1). Moreover, the positive correlation between the annual ET_0 and VP-NDVI ($R = 0.29$) reflects potential influence of the thermal condition on the grass growth in this sub-humid area of the NTP (see Figure 5).

Sokshan County

Climatically, Sokshan County is located in the sub-frigid zone, but the annual precipitation is less than that of Chali station. In this region, a positive correlation ($R=0.53$, $p<0.05$) between VP-NDVI and precipitation during grass growth period (from July to September) argued that moisture condition is a limiting factor for vegetation growth in Sokshan region.

Shantsa County

Climatically, Shantsa County is located in the frigid arid zone. The annual mean wind velocity of Shantsa County exceeds 4.5 m/s, which is the largest in six counties of the NTP. The correlation coefficient between annual mean wind velocity and VP-NDVI is negative ($R = -0.40$, $p<0.05$). It is conceivable that VP-NDVI is affected by wind velocity and transpiration rate. Normally, grassland degradation and desertification include a series of processes, i.e., wind erosion, sand stream, shifting sand-dune and accumulation and sand-dune migration [53]. In the mean time, the correlation coefficients between ET_0 and VP-NDVI is negative for Shantsa ($R = -0.51$, $p<0.05$). The cold, dry, windy climatic conditions along with high potential evaporation affect the grass growth in this region. With the increase of the ET_0 , the vegetation stress increases, therefore inhibiting the vegetation growth. The increase of ET_0 in the frigid arid zone of the NTP, owing to an increase in temperature and decrease in humidity, leads to further degradation of the grassland and promotes the occurrence and development of desertification over these areas. Yang et al. (1998) also reported that high evaporative demand in grow season often results in soil moisture depletion, and thereby, adversely affecting grassland growth in the U.S. Great Plains regions [44].

Palgon and Amdo counties

Palgon and Amdo counties are located in sub-frigid and sub-arid region. A positive relationship between VP-NDVI and precipitation (from July to September) for Palgon County ($R = 0.39$) indicated that precipitation is responsible for the observed fluctuation in VP-NDVI. Table 3 showed that the little long-term trend of both NDVI and rainfall ($b_v = 0.058$, $b_p = 0.067$) in Palgon County. In Amdo County, the negative correlation between VP-NDVI and T_{\min} ($R = 0.47$, $p<0.05$), indicated that, to some extent, the minimum temperature is the main effecting factor on grass growth in this area. The correlation coefficients between ET_0 and VP-NDVI are negative for Palgon ($R = -0.63$, $p<0.01$) and Amdo ($R = -0.54$, $p<0.05$), which also showed the benefit of decreasing potential ET to the vegetation growth.

4.3 NDVI and anthropogenic driving force

The human activity is an important driving force that affects vegetation condition in the NTP. Table 6 shows that the Sokshan County has the highest population density in the NTP, while the Chali County has the highest rate in population growth. In eastern NTP, livestock grazing is one important sector of the local economy [2]. It is generally believed that grassland degradation is mainly caused by human's improper usage of the land, such as over-grazing. At the end of 2003, the total number of livestock on hand in the NTP was 7.682 million, nearly a two-fold increase over that of 1958 [7].

Table 6. Population density (person km⁻²) in the 2002 census and the population change (%) in six counties from 1989 to 2002.

County	Nak chu	C hali	A mdo	Sha ntsa	Soks han	Pal gon
Population density in 2002 (persons km ⁻²)	5.14	1.93	1.30	0.42	5.94	0.33
Population change (%) 1989-2002	23.12	24.33	17.15	20.44	21.49	22.68

Population of the Sokshan County has increased from 19,371 in 1989 to 23,694 in 2000 [54], whereas the NDVI has decreased in this time period (see Figure 5). The correlation coefficient (R) between VP-NDVI and population from 1981 to 2001 for six counties in the NTP was shown in Table 7.

Table 7. The correlation coefficient (R) between VP-NDVI and population from 1981 to 2001 for six counties in the NTP.

County	Nakchu	Shantsa	Palgon	Amdo	Sokshan	Chali
R	0.26	0.25	-0.24	-0.06	-0.40*	-0.45*

* Correlation is significant at 0.05 level

The negative correlation between the VP-NDVI and population ($R = -0.40$, $p < 0.05$) implied that human activities have played a role in causing grassland degradation in Sokshan County. Likewise, a negative correlation between the VP-NDVI and population in the Chali County ($R = -0.45$, $p < 0.05$) indicated the adverse impact of human activity. The two counties (Chali and Sokshan) with significant negative VP-NDVI and population relationships occur in the region, which has high decrease VP-NDVI slope values in Figure 3. In contrast, weak relationships between VP-NDVI and population were observed in Shantsa, Palgon and Amdo counties, all of which belong to the semi-arid, sub-frigid, and frigid-arid zone in central and eastern-central NTP. The weak relationship pointed out that the climate and environmental condition, rather than human impact, is mainly responsible for the grassland degradation occurred in those areas.

5. Conclusions

Monitoring and quantifying dynamics and spatial variability of the grassland ecosystems of the world is crucial for understanding and mitigating the grassland degradation caused by natural and anthropogenic forces. The study reported here has revealed the long-term temporal and spatial

variations of one unique grassland ecosystem in the Northern Tibetan Plateau (NTP) and the possible driving forces during 1981 to 2001.

A long-term trend of VP-NDVI was analyzed by using linear regression. A moderate to high increase of VP-NDVI from 1981 to 2001 has occurred in the east part of the NTP, which is located at the low altitude zone (Nakchu, Shantsa, and Palgon counties). In contrast, a moderate decrease in VP-NDVI has occurred in the east-central part of the NTP over the same period (Amdo, Sokshan and Chali counties). The increasing population and human activities in Sokshan and Chali counties have resulted in grassland degradation during the latter part of the 20th century. Areas with slight-decrease or no-change of VP-NDVI were found in the western part of the NTP, which is dominated by alpine grassland and alpine desert grassland (Nima and Shuanghu counties). The weak decline in VP-NDVI in this area is not likely caused by human activities because these two counties have very little human settlement.

A statistical analysis was carried out to study relationship between VP-NDVI and climate variables. Climatically, Nakchu, Shantsa, Palgon and Amdo counties are located in the sub-frigid semi-arid zone. In Nakchu and Amdo counties, T_{\min} is found to be a major limiting factor on over-wintered perennial grass; increased T_{\min} from 1980s to 2000 has benefited the grassland growth. In Palgon County, precipitation is found responsible for observed VP-NDVI fluctuations from 1981 to 2001. The negative correlations between ET_0 and VP-NDVI obtained for Nakchu, Shantsa, Palgon and Amdo counties indicate that high potential evaporation can negatively impact grassland growth. Overall, increases of ET_0 in the sub-frigid, semi-arid and frigid-arid zone of the NTP, owing to increase in temperature and decrease in humidity, have led to degradation of the grassland and the development of desertification in these area.

Significant shifts in climatic conditions and continued human alteration through land use and other activities will certainly affect natural grassland ecosystems of the world, especially in regions which are very sensitive to climate change (e.g. arid and semiarid and alpine regions) [55].

Although this study mainly reveals some uneven alterations of the grassland and some significant correlations between the grassland dynamics and degradation and the possible driving forces related to climate and anthropogenic activities in the NTP in an interannual scale. However, the interannual interval can partially describe the complex dynamics of grassland and it's related to the climatic factors in the NTP. The different intervals and the possible physical mechanisms responsible for the feedback of grassland dynamics and degradation in this region need to be further studied.

Acknowledgments

This work was supported jointly by the Ministry of Science and Technology of China Project (Grant No.2003DIB4J144, 2006GB24160430), The National Natural Science Foundation of China (Grant No.30370814, 40641003), China Meteorological Administration Climate Change Project (Grant No.CCSF2007-4), and The Foundation of the Key Laboratory of Land Use, The Ministry of Land and Resources, China (No.07-01). We thank three anonymous reviewers for their constructive and critical comments on the manuscripts.

References

1. Ye, D.Z.; Gao, Y.X. *Meteorology of the Qinghai-Xizang Plateau*; Beijing: Science Press.1979; pp 279.
2. Liu, S.Z.; Zhou, L.; Qiu, C.S.; Zhang, J.P.; Fang, Y.P.; Gao, W.S. *Studies on Grassland Degradation and Desertification of Naqu Prefecture in Tibet Autonomous Region*; People's Press: Lhasa, Tibet: 1999; pp 4-33.
3. Sun, H.L.; Zheng, D. *Formation, evolution and development of Qinghai-Xizang Plateau*. Guang Zhou: Guang Dong Scientific and Technological Press. 1998; pp 66-148.
4. An, Z.S.; Kutzbuch, J.E.; Prell, W.L.; Porter, S.C. Evolution of Asian monsoons and phased uplift of the Himalaya Tibetan plateau since Late Miocene times. *Nature* **2001**, *411*,62-66.
5. Su, D.; Xue, S. *Grassland Resources in Tibet Autonomous Region*. Science Press: Beijing, 1994; pp189–193.
6. Ye, D.; Wu, G. The role of the heat source of the Tibetan Plateau in the general circulation. *Meteor. Atmos. Phys.* **1998**, *67*, 181-198.
7. Liu, X.S.; Ma, Y.C.; La, B.; Yu, Z.S. *Climatic Division of the Animal Husbandry of Naqu Region*. Meteorological Press: Beijing, China, 2003; pp 6-34.
8. Zhang, J.H.; Dong, W.J.; Wang, C.Y.; Liu, J.Y.; Yao, F.M. Dynamic of China's cultivated land and land cover changes of its typical regions based on remote sensing data. *J. Fore. Res.* **2001**, *12*, 183-186.
9. Vitousek, P.M.; Mooney, H.A.; Lubchenco, J.; Melillo,J.M. Human domination of Earth's ecosystems. *Science* **1997**, *277*, 494–499.
10. Geist, H.; Lepers, E.; McConnel, W.; Lambin, E.; Ramankutty, N. Land-Use and Land-Cover Change/Meta-analyses of the causes and synthesis of the rates of change. *IHDP, UPDATE* **2002**, *4*, 15.
11. Zhang J.H.; Bian L.G.; Liu X.S. To study eco-environment and meteorological disasters in Northern Tibet-Plateau based on remote sensing information. *J. Mountain Sci.* **2005**, *23*, 94-100.
12. Fang, X.; Han, Y.; Ma, J.; Song, L.; Yang, S.; Zhang, X. Dust storms and loess accumulation on the Tibetan Plateau: A Case study of dust event on 4 March 2003 in Lhasa. *Chin. Sci. Bull.* **2004**, *49*, 953-960.
13. Matthews, E. Global vegetation and land use: New high resolution data bases for climate studies. *J. Climatol. Appl. Meteorol.* **1983**, *22*, 474-487.
14. Tucker, C.J.; Justice C.O. Satellite remote sensing of primary production. *Int. J. Remote Sens.* **1987**, *7*, 1395-1416.
15. Gutman, G. On the relationship between monthly mean and maximum value composite normalized vegetation indices. *Int. J. Remote Sens.* **1989**, *10*, 1317-1325.
16. Paul, T. Remote sensing technology for rangeland management applications. *Int. J. Range Manag.* **1989**, *42*, 1-14.
17. Plummer, S.E. Perspectives on combining ecological process models and remotely sensed data. *Ecol. Model.* **2000**, *129*, 169-186.
18. García, M.; Villagarcía, L.; Contreras, S.; Domingo, F.; Puigdefábregas, J. Comparison of three operative models for estimating the surface water deficit using ASTER reflective and thermal data. *Sensors* **2007**, *7*, 860-883.
19. Taylor, B.F. Determination of seasonal and inter-annual variation in New Zealand pasture growth

- from NOAA-7 Data. *Remote Sens. Environ.* **1985**, *18*, 177-192.
20. Cihlar, J.; St-Laurent, L.; Dyer, J.A. Relation between the normalized difference vegetation index and ecological variables. *Remote Sens. Environ.* **1993**, *35*, 279-298.
 21. Ehlich, D.; Estes, J.E.; Singh, A. Application of NOAA-AVHRR 1km data for environmental monitoring. *Int. J. Remote Sens.* **1994**, *15*, 145-161.
 22. Csizsar, I.; Gutman, G. Mapping global land surface albedo from NOAA AVHRR. *J. Geophys. Res.* **1999**, *104*, 6215-6228.
 23. Zhang, J.H.; Fu, C.B.; Kanzawa, H. Simulating canopy stomata conductance of winter wheat and its distribution using remote sensing information. *J. Environ. Sci.* **2001**, *13*(4), 439-443.
 24. Shabanov, N.V.; Zhou, L.; Knyazikhin, Y.; Myneni, R.B.; Tucker, C.J. Analysis of Inter-annual Changes in Northern Vegetation Activity Observed in AVHRR Data From 1981 to 1994. *IEEE. Trans. Geosci. Remote Sens.* **2002**, *40*, 115-130.
 25. Tucker, C.J.; Townshend, J.R.G.; Goff, T.E. African land-cover classification using satellite data. *Science* **1985**, *227*, 369-375.
 26. Justice, C. Monitoring the grasslands of semi-arid Africa using NOAA-AVHRR data. *Int. J. Remote Sens.* **1986**, *7*, 1383-1622.
 27. Townshend, J.R.G. Global data sets for land applications from the advanced very high resolution radiometer: an introduction. *Int. J. Remote Sens.* **1994**, *15*, 3319-3332.
 28. Eidenshink, J.C.; Faundeen, J.L. The 1 km AVHRR global land data set: First stages of implementation. *Int. J. Remote Sens.* **1994**, *15*, 3343-3462.
 29. Defries, R.S.; Hansen, M.; Townshend, J.R.G. Global discrimination of land cover types from metrics derived from AVHRR pathfinder data. *Remote Sens. Environ.* **1995**, *54*, 209-222.
 30. Gutman, G.; Ignatov, A. Global land monitoring from AVHRR: Potential and limitations. *Int. J. Remote Sens.* **1995**, *16*, 2301-2309.
 31. Running, S.W.; Loveland, T.R.; Pierce, L.L.; Nemani, R.R.; Hunt, E.R.J. A remote sensing based vegetation classification logic for global land cover analysis. *Remote Sens. Environ.* **1995**, *51*, 39-48.
 32. Loveland, T.R.; Reed, B.C.; Brown, J.F.; Ohlen, D.O.; Zhu, Z.; Yang, L.; Merchant, J.W. Development of a global land cover characteristics database and IGBP DIS cover from 12km AVHRR data. *Int. J. Remote Sens.* **2000**, *21*, 1303-1330.
 33. Stow D. A.; Hope, A.; McGuire, D.; Verbyla, D.; Gamon, J.D.; Daeschner, S.; Petersen, A.; Zhou L.; Myneni, R. Remote sensing of vegetation and land-cover change in Arctic Tundra Ecosystems. *Remote Sens. Environ.* **2004**, *89*, 281-308.
 34. Kogan, F.N. Remote sensing of weather impacts on vegetation in non-homogeneous area. *Int. J. of Remote Sens.* **1990**, *11*, 1405-1419.
 35. Anyamba, A.; Eastman, J.R. Interannual Variability of NDVI over Africa and its Relation to EL Nino/Southern Oscillation. *Int. J. Remote Sens.* **1996**, *17*, 2533-2548.
 36. Gutman, G.G. Global data on land surface parameters from NOAA AVHRR for use in numerical climate models. *J. Clim.* **1994**, *7*, 669-680.
 37. Moulin, S.; Kergoat, L.; Viovy, N.; Dedieu, G.G. Global-scale assessment of vegetation phenology using NOAA/ AVHRR satellite measurements. *J. Clim.* **1997**, *10*, 1154-1170.
 38. Goetz, S.J. Multi-sensor analysis of NDVI, surface temperature and biophysical variable at a mixed grassland site. *Int. J. Remote Sens.* **1997**, *18*, 71-94.
 39. Los, S.O.; Collatz, G.J.; Sellers, P.J.; Malmstrom, C.M.; Pollack, N.H.; Defries, R.S.; Bounoua,

- L.; Parris, M.T.; Tucker, C.J.; Dazlich, D.A. A global 9-yr biophysical land surface dataset from NOAA AVHRR Data. *J. Hydrometeorol.* **2000**, *1*, 183-199.
40. Zhang, J.H.; Yao, F.M.; Fu, C.B.; Yan, X.D. Study on response of ecosystem to the East Asian monsoon in eastern China using LAI data derived from remote sensing information, *Prog. Nat. Sci.* **2004**, *14*, 279-282.
41. Braswell, B.H.; Schimel, D.S.; Linder, E.; Moore, III, B. The response of global terrestrial ecosystems to interannual temperature variability. *Science*. **1997**, *278*, 870-873.
42. Shaw, M.R.; Zavaleta, E.S.; Chiariello, N.R.; Cleland, E.E.; Mooney, H.A.; Field, C.B. Grassland responses to global environmental changes suppressed by elevated CO₂. *Science* **2002**, *298*, 1987-1990.
43. Zavaleta, E.S.; Shaw, M.R.; Chiariello, N.R.; Thomas, B.D.; Cleland, E.E.; Field, C.B.; Mooney, H.A. Grassland responses to three years of elevated temperature, CO₂, precipitation, and N deposition. *Ecol. Monog.* **2003**, *73*, 585-604.
44. Yang, L.; Wylie, B.K.; Tieszen, L.L.; Reed, B.C. An analysis of relationships among climate forcing and Time-integrated NDVI of grasslands over the U.S. Northern and Central Great Plains: *Remote Sens. Environ.* **1998**, *65*, 25-37.
45. Zhang, R.Z.; Zheng, D.; Yang, Q.Y. *A Physical Geography of Tibet*. Science Press: Beijing, China 1982; 178 pp.
46. Agbu, P.A.; James, M.E. *The NOAA/NASA Pathfinder AVHRR Land Data Set User's Manual*. Goddard Distributed Active Archive Center, NASA, Goddard Space Flight Center, Greenbelt, 1994.
47. Rao, C.R.N.; Chen, J. Revised post-launch calibration of the visible and near-infrared channels of the Advanced Very High Resolution Radiometer on the NOAA-14 spacecraft. *Int. J. Remote Sens.* **1999**, *20*, 3485-3491.
48. Holben, B.N. Characteristics of maximum-value composite images from temporal AVHRR data. *Int. J. Remote Sens.* **1986**, *7*, 1417-1434.
49. Myneni, R.B.; Hall, F.G.; Sellers, P.J.; Marshak, A.L. The interpretation of spectral vegetation indexes. *IEEE Trans. Geosci. Rem. Sens.* **1995**, *33*, 481-486.
50. Runnström, M.C. Is northern China winning the battle against desertification?: Satellite remote sensing as a tool to study biomass trends on the Ordos Plateau in semiarid China. *AMBIO* **2000**, *29*(8), 468-476.
51. Allen, R.G.; Pereira, L.S.; Raes, D.; Smith, M. *Crop evapotranspiration. FAO Irrigation and Drainage*. Paper 24, Rome. Italy, 1998; 290p.
52. Liu, X.D.; Chen, B. Climate warming in the Tibetan Plateau during recent decades. *Int. J. Climatol.* **2000**, *20*, 1729-1742.
53. Zhang G.P.; Zhang, J.H.; Sun Z.X. Quantitative study on Aeolian erosion of soil in China based on GIS/RS techniques. *J. Mountain Science*, **2005**, *23*(suppl.), 117-123.
54. Nakchu Statistical Bureau. *The Corpus of Statistical Data of Nakchu Prefecture in Tibet Autonomous Region (1958-2000)*. Lhasa: Tibet Statistical Press. 2001.
55. Beniston, M. Climatic change in mountain regions: a review of possible impacts. *Clim. Change* **2003**, *59*, 5-31.